

Supporting Information

C-terminal truncated α -synuclein fibrils contain strongly twisted β -sheets

Aditya Iyer^{†‡}, Steven J. Roeters^{†||}, Vladimir Kogan¹, Sander Woutersen^{*‡}, Mireille M.A.E
Claessens^{*‡} and Vinod Subramaniam^{*†‡¥}

[†]Nanoscale Biophysics Group, AMOLF, Science Park 104, Amsterdam 1098 XG, The
Netherlands.

[‡]Van 't Hoff Institute for Molecular Sciences, University of Amsterdam, Science Park 904,
Amsterdam 1098 XH, The Netherlands.

[‡]Nanobiophysics Group, MESA+ Institute for Nanotechnology, University of Twente,
Drienerlolaan 5, Enschede 7522 NB, The Netherlands.

¹Dannalab BV, Wethouder Beversstraat 185, Enschede 7543 BK, The Netherlands

[¥]Vrije Universiteit Amsterdam, De Boelelaan 1105, Amsterdam 1081 HV, The Netherlands

^{||}Both authors contributed equally to the presented work.

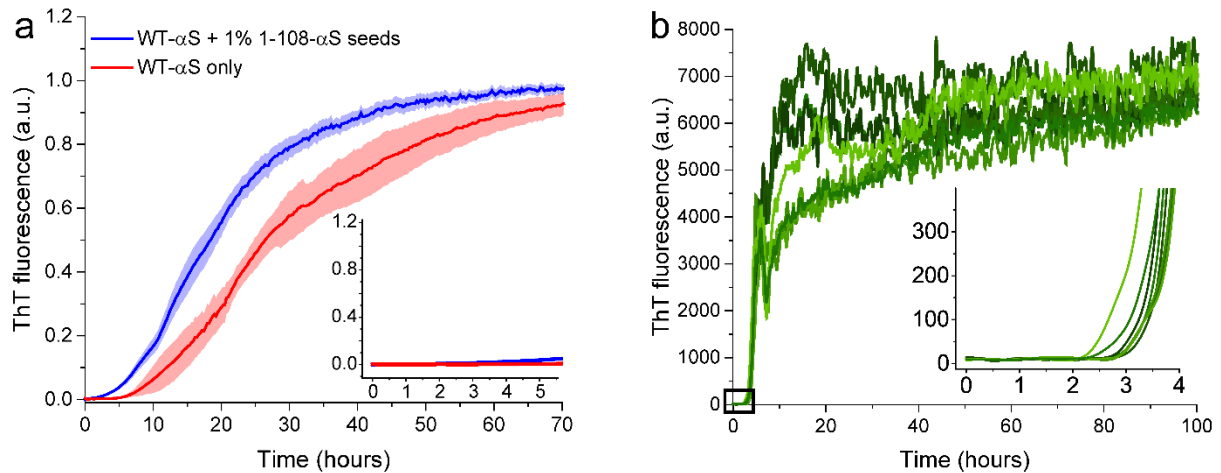


Figure S1: Comparison of aggregation curves of unseeded WT- α S monomers and those in presence of 1% 1-108- α S seeds. In presence of 1-108- α S seeds, WT- α S monomers show a smaller lag-time compared to unseeded WT- α S monomers (a). Shaded regions in panel a indicate s.d. from an aggregation experiment with at least 6 replicates. Unseeded aggregation curves of 1-108- α S fibrils (b). 35 μ M of monomeric protein was allowed to aggregate (8 replicates) in PBS buffer at 37 $^{\circ}$ C in a fluorescence microplate reader. The inset shows the first 4 hours of aggregation. In the absence of any added seeds, 1-108- α S monomers aggregated with a finite lag time of \sim 3 hours which disappeared in presence of either WT- α S or 1-108- α S seeds (see **Fig. 1b/c** in main text) suggesting that the nucleation is indeed bypassed for 1-108- α S monomers. Prior to aggregation assays, the protein sample was filtered using a 100 kDa membrane to get rid of any pre-existing aggregates and protein concentration was estimated using UV absorbance at 276 nm. Data-points were recorded every 15 minutes. ThT concentration was 5 μ M.

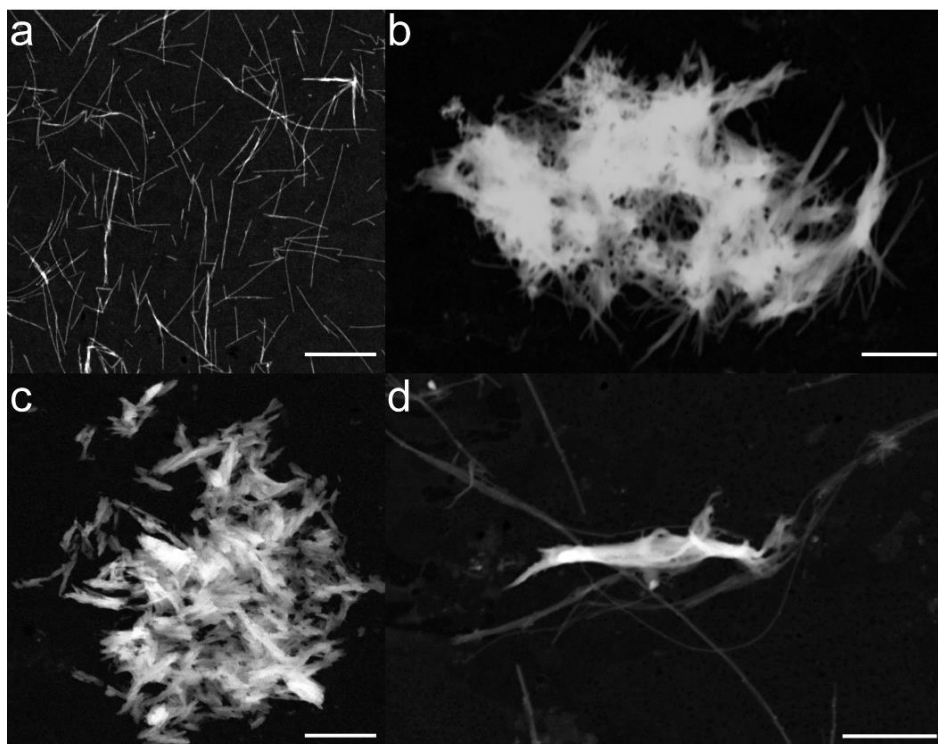


Figure S2: STEM images of homologous and heterologous seeded fibrils of WT- α S and 1-108- α S. Representative scanning-transmission electron microscopy (STEM) micrographs of α S fibrils from seeding of WT- α S monomers with WT- α S seeds (**a**), 1-108- α S monomers with WT- α S seeds (**b**), 1-108- α S monomers with 1-108- α S seeds (**c**) and WT- α S monomers with 1-108- α S seeds (**d**) respectively. Homologous seeding showed elongated rod-like fibrils for WT- α S and higher-ordered aggregates of 1-108- α S fibrils (panel **a/c**). Heterologous seeding of 1-108- α S monomers with WT- α S seeds also showed higher-ordered fibrillar aggregates. Heterologous seeding of WT- α S monomers with 1-108- α S seeds resembled WT- α S fibrils (panel **d**) which we believe were formed predominantly from WT- α S monomers only. The high intensity aggregate in the center of panel **d** is a 1-108- α S seed as quantified by mass-mapping using high-angle annular dark-field (HAADF) detectors in the STEM microscope. Compared to WT- α S fibrils, the 1-108- α S seeds show a ~ 5 -fold higher intensity allowing us to discern WT- α S and 1-108- α S fibrils. The seed concentration was 1% (v/v). Fibrils were imaged at the plateau stage of seeded aggregation curves (red arrows in **Fig. 1** of main text). Scale bar in all panels in 0.5 μ m.

Supporting discussion on differential absorption flattening (DAF)

Differential absorption flattening (DAF) is a phenomenon that leads to peak shifts in the UV-CD spectrum of solutions that contain a non-random distribution of chromophores with dimensions greater than $1/20^{\text{th}}$ the wavelength of the probe light. To ascertain whether DAF effects were present in 1-108- α S fibrils, UV-CD spectra and STEM micrographs were obtained for both settled and suspended 1-108- α S fibrils (**Supporting Fig. S3**). When DAF effects are significant, a peak shift in the suspended fibrils with respect to the settled fibril pellet is expected, as the latter contains a larger amount of settled aggregated fibrils relative to isolated fibrils. The UV-CD spectra exhibit no peak shifts, which means that the CD spectral differences between WT- α S and 1-108- α S fibrils cannot be caused by DAF effects. Additional evidence for the unlikelihood of DAF effects or differential scattering can be found with another truncation variant of α S lacking residues 125-140 (henceforth 1-124- α S)¹. Although STEM micrographs confirmed the presence of higher-ordered aggregates of 1-124- α S fibrils, their UV-CD spectra are much less perturbed with respect to the WT- α S fibrils (**Supporting Fig. S4**). Thus, the presence of higher-ordered aggregates of α S fibrils does not *per se* result in the observed differences in the UV-CD spectra, and DAF effects, if present in the aggregated 1-108- α S fibril suspensions, are minimal.

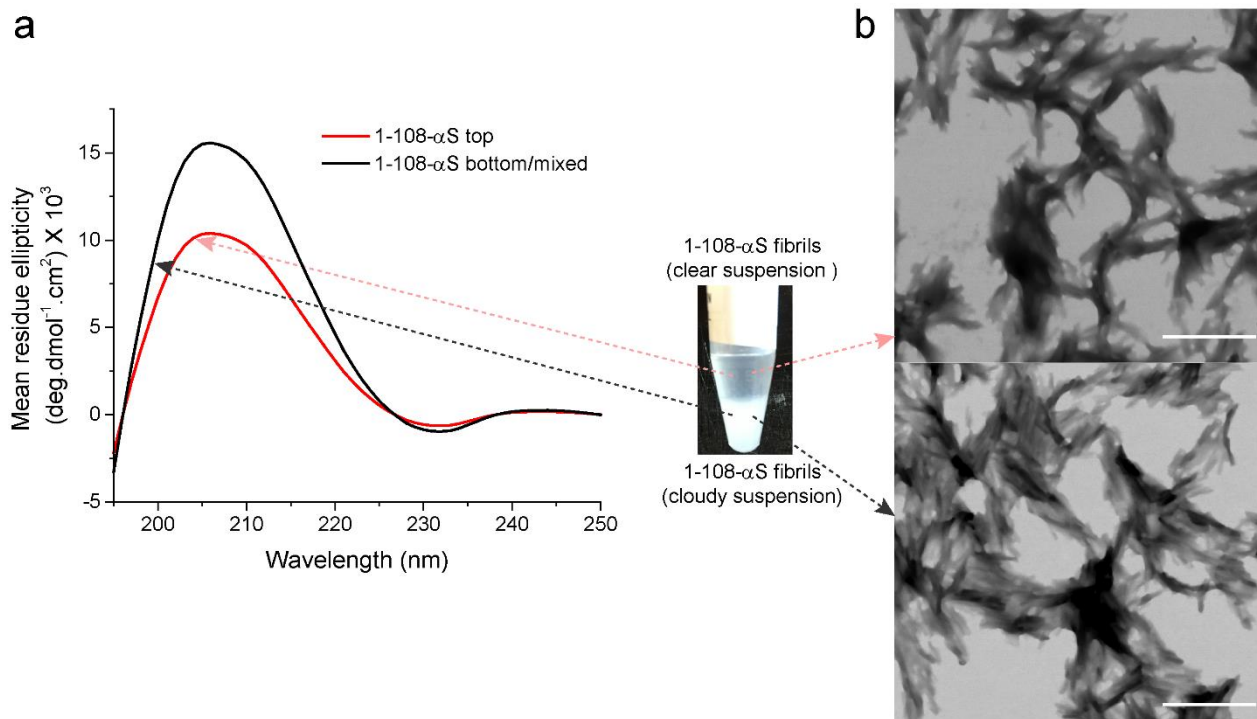


Figure S3: CD spectra (**a**) and corresponding STEM micrographs (**b**) of 1-108- α S fibrils obtained from settled and suspended regions in the tube. The scale bar is 0.5 μ m. A decrease in the CD signal between these two samples is due to a decreased concentration of fibrils. Negligible changes in the peak positions exclude DAF effects to be the likely cause.

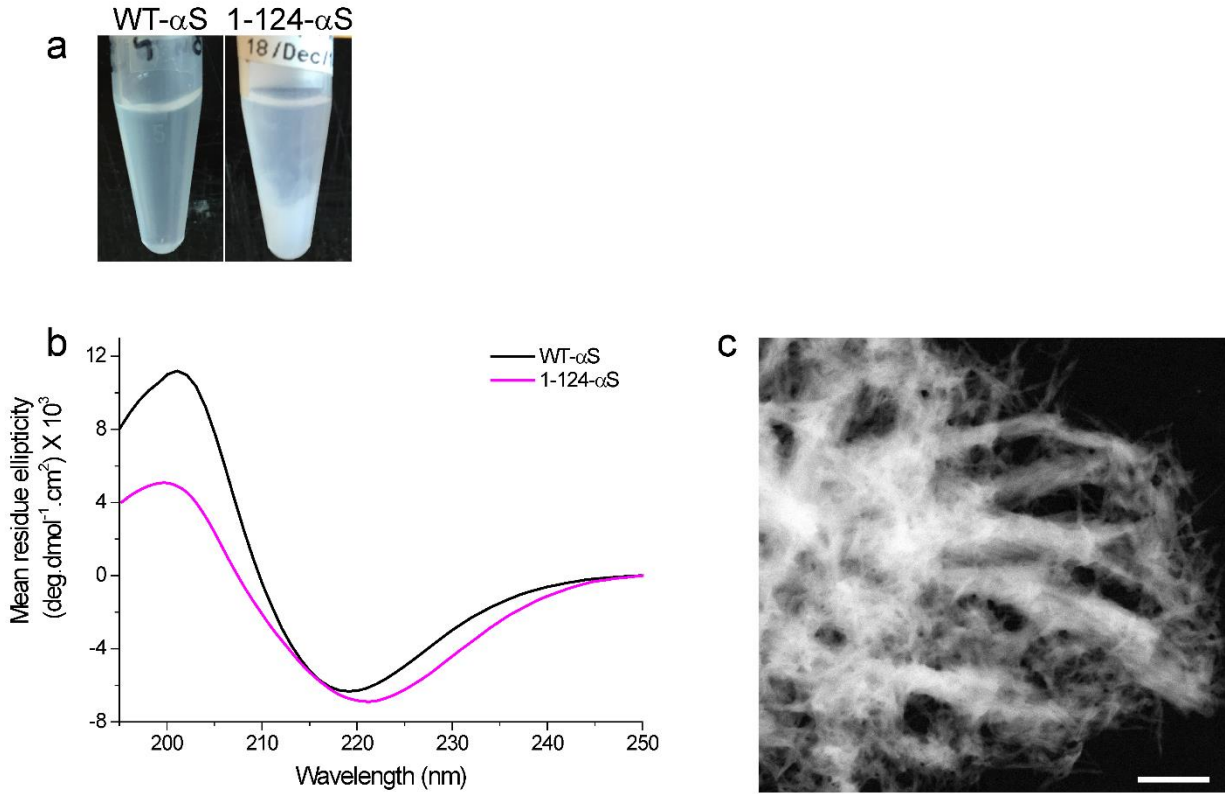


Figure S4: Images of aggregated suspensions of WT- α S and 1-124- α S fibrils in Eppendorf tubes when left unperturbed for several hours (a). Aggregated 1-124- α S also settle down forming distinct clear and cloudy phases similar to aggregated 1-108- α S. CD spectra (pink line, b) and corresponding STEM micrographs of a suspension of 1-124- α S fibrils (c). The scale bar is 0.5 μ m. All measurements were performed at room temperature.

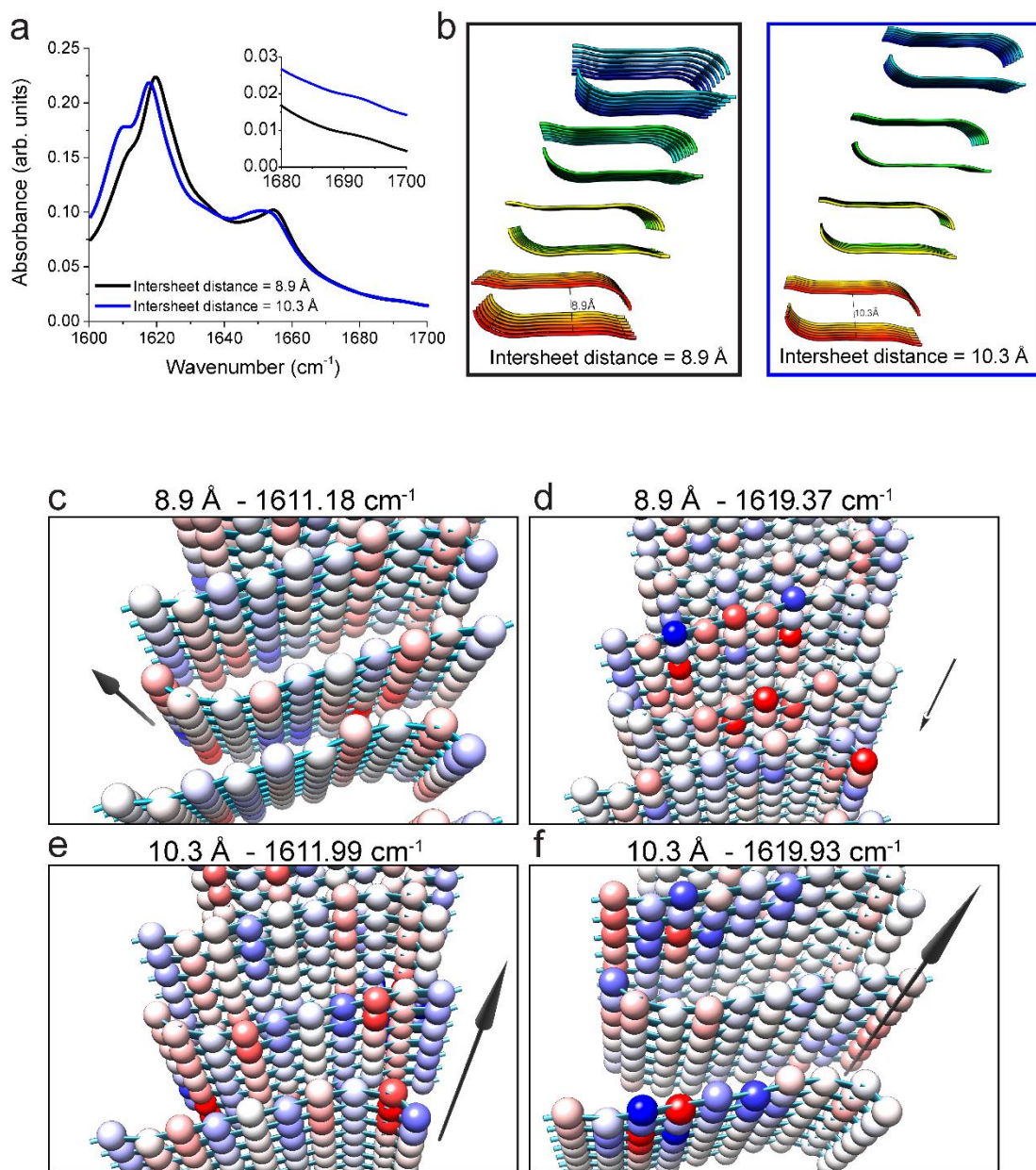


Figure S5: Calculated IR spectra of WT- α S fibrils (black) and 1-108- α S fibrils (blue) (a). Both spectra are calculated with a local-mode frequency of 1646 cm^{-1} and a homogeneous linewidth of 4.5 cm^{-1} . The one-exciton Hamiltonian is constructed according to the formalism described previously² for the α S-like fibrillar structures depicted in (b). The WT- α S-like structure is exactly the unit cell of PDB entry 4RIL extended into 7 monomers along the fibril axis and 8 monomers perpendicular to this axis. The 1-108- α S like structure used

in the calculations was created by increasing the inter-sheet distance according to the difference found in the XRD spectra. The spectra depicted in (a) show that the broadening of the low-frequency peak can only partly be explained by the increased inter-sheet distance; to fully describe the spectral changes an additional spectral broadening has to be taken into account (see **Fig. 3a** in main text) that is probably due to and increased presence of water in the 1-108- α S fibril. The presence of the turn in the last 2 residues is vital for a proper reproduction of the peaks in the experimental spectra, as removal of the last residue, Ala 78, results in a much weaker 1657 cm^{-1} peak, indicating that turns are indeed in part the origin of this peak, in line with the simulations presented in ref. 3 for other amyloid structures (without the turn residues there is still a peak at this frequency which is hence probably a β -sheet mode as well). A Lorentzian with a central frequency of 1632 cm^{-1} and a width of 30 cm^{-1} was added such that the ratio of the total spectral intensity of the random coil and the non-random coil residues was consistent with the secondary structure assignment of the residues as found by ss-NMR⁴. As Ref. 4 reports that residue 16-20 and 37-94 are in β -sheet or turn conformation, while the other residues obtain a random-coil conformation for the employed salt conditions, a ratio of 1.22 and 0.75 is used for the WT- α S and 1-108- α S spectrum, respectively. (c-f) A normal-mode analysis of the strongest modes ($\sim 1620\text{ cm}^{-1}$) and the low-frequency shoulders ($\sim 1610\text{ cm}^{-1}$) for both structures depicted in (b), with the direction and size of the respective normal modes depicted by the gray arrow. The analysis reveals that, although the $\sim 1620\text{ cm}^{-1}$ modes look similar (the proximity of neighboring intermolecularly hydrogen-bonded β -sheets seems to influence these normal modes heavily, as the in-phase behavior along the hydrogen-bonding axis that is typical for the strongest mode of an isolated β -sheet^{5,6}, v_{\perp} , is absent in these cases), the $\sim 1610\text{ cm}^{-1}$ modes are different for the two structures: while this mode is also influenced by the neighboring sheets in the tightly stacked case (left image in (b)), in the more extended structure (right image in (b)) this influence appears to be less strong, resulting in a 1.7 times as strong normal mode in which all amide-I oscillators oscillate in phase along the hydrogen-bonding axis.

Supporting References

- (1) Hoyer, W.; Cherny, D.; Subramaniam, V.; Jovin, T. M. *Biochemistry* **2004**, *43*, 16233-16242.
- (2) Roeters, S. J.; van Dijk, C. N.; Torres-Knoop, A.; Backus, E. H.; Campen, R. K.; Bonn, M.; Woutersen, S. *J. Phys. Chem. A* **2013**, *117*, 6311-6322.
- (3) Karjalainen, E. L.; Ravi, H. K.; Barth, A. *J. Phys. Chem. B* **2011**, *115*, 749-757.
- (4) Gath, J.; Bousset, L.; Habenstein, B.; Melki, R.; Bockmann, A.; Meier, B. H. *PLoS One* **2014**, *9*, e90659.
- (5) Abramavicius, D.; Mukamel, S. *J. Chem. Phys.* **2004**, *120*, 8373-8378.
- (6) Ganim, Z.; Chung, H. S.; Smith, A. W.; Deflores, L. P.; Jones, K. C.; Tokmakoff, A. *Acc. Chem. Res.* **2008**, *41*, 432-441.